View metadata, citation and similar papers at core.ac.uk
brought to you by CORE
provided by Repository@USM

COMPLEX COACERVATED MICROCAPSULES IN CREAM FOR TOPICAL DELIVERY OF THE CURCUMINOIDS AND QUERCETIN

ANG LEE FUNG

UNIVERSITI SAINS MALAYSIA

2015

COMPLEX COACERVATED MICROCAPSULES IN CREAM FOR TOPICAL DELIVERY OF THE CURCUMINOIDS AND QUERCETIN

by

ANG LEE FUNG

Thesis submitted in fulfillment of the requirements for the degree of Doctor of Philosophy

December 2015

ACKNOWLEDGEMENTS

Studying for this PhD degree was made possible by commitment from individuals, organizations and institutions. It is vital that I acknowledge their assistance, contribution and commitment.

This thesis owes its existence to the help, support, and inspiration of many people. In the first place, I would like to express my sincere appreciation and gratitude to my supervisor, Associate Prof. Dr. Yusrida Darwis for her unlimited support and encouragement during the past five years of my research. She has provided an optimum working environment at the Department of Pharmaceutical Technology, School of Pharmaceutical Sciences, Universiti Sains Malaysia. Her perpetual energy and enthusiasm in research had motivated all her advisees, including me. In addition, she was always accessible and willing to help her students with their research. As a result, research life became smooth and rewarding for me. Her uncompromising quest for excellence significantly shapes everyone at the department.

I wish to express my sincere appreciation and gratitude to my co-supervisor, Associate Prof. Dr. Yvonne Tan Tze Fung for her guidance, help and patience.

I am also indebted to Dr Koh Rhun Yian, who has not only been a source of enthusiasm and encouragement, but has also agreed, with her exceptional insights into cell culture, to serve and enrich my knowledge in the *in vitro* part of my research.

All my lab buddies at the Pharmaceutical Technology Department made it a convivial place to work. In particular, I would like to thank Ms. Nor Atiqah, Mr. Arshad, Ms. Nor Azah, Mr. Jahanzeb, Ms. Reem, Mr. Ibrahim Ms. Madeeha and Ms. Thiruchelvi.

Collective and individual acknowledgments are also owed to all the technical and non-technical staff of the School of Pharmaceutical Sciences, Universiti Sains Malaysia. Many thanks go in particular to Mr. Samsuddin, Mr. Roseli Hassan, Mr. Basri Jaafar, Mr. Ibrahim, Ms. Salida, Mr. Amiruddin and Mr. Azrollyzam.

I have greatly appreciated the generous financial support from The Ministry of Science and Technology Malaysia (MOSTI) who provided the National Science Fellowship (NSF) for my study.

My deepest gratitude goes to my family for their unflagging love and support throughout my life; this dissertation is simply impossible without them. I want to thank my late father, Mr. Ang Ah Hua, for his care and love. I cannot ask for more from my mother, Mrs. Teng Boay Kee, as she is simply perfect. I have no suitable word that can fully describe her everlasting love to me. I am also grateful to my partner, Dr. M. F. Yam who was always my support in the moments when where was no one to answer my queries.

Ang Lee Fung

TABLES OF CONTENTS

Acknowledgement		ii
Table of Contents		iv
List of Tables		xiii
List of Figures		xvii
List of Plates		xxiv
List of Abbreviations		xxvii
List of Appendices		xxix
Abstrak		xxx
Abstract		xxxii

CHAPTER 1 - INTRODUCTION

1.1	Active ingredients		1
	1.1.1	Curcuminoids/curcumin	1
	1.1.2	Quercetin	4
1.2	Microencapsulation		6
	1.2.1	Introduction of microencapsulation	6
	1.2.2	Core material	9
	1.2.3	Coating material	9
		1.2.3 (a) Gelatin	10
		1.2.3 (b) Chitosan	14
	1.2.4	Crosslinking agent	16
		1.2.4 (a) Formaldehyde crosslinking mechanism	17
	1.2.5	Classification of microcapsules and microspheres	19
	1.2.6	Coacervation microencapsulation	20
		1.2.6 (a) Complex coacervation systems	20
		1.2.6 (b) Complex coacervation microencapsulation process	21
	1.2.7	Release mechanism of microcapsules	25
	1.2.8	Advantages of microencapsulation	27
	1.2.9	Application of microcapsules to end product	28
	1.2.10	Microcapsule controlled drug delivery system	29

1.3 Topical drug delivery 29
1.3.1 Cream and emulsion 30
1.3.1 (a) Surfactant and the HLB system 31
1.3.1 (b) Characterization of cream 34
1.3.1 (c) Stability of cream 37
1.4 Wound healing 40
1.4.1 Wound and wound types 40
1.4.2 Degree of wound 41
1.4.3 Degree of burn wound 42
1.4.4 Mechanisms of wound healing 42
1.5 Statement of the problem 44
1.6 Objectives 44

CHAPTER 2 - HPLC METHOD DEVELOPMENT AND VALIDATION FOR SIMULTANEOUS DETERMINATION OF QUERCETIN AND CURCUMINOIDS
2.1 Introduction 46
2.2 Materials and methods 49
2.2.1 Materials 49
2.2.2 Methods 50
2.2.2.1 HPLC instrumentation 50
2.2.2.2 Chromatographic conditions 50
2.2.2.3 Preparation of standard and quality control solutions 50
2.2.2.4 Limit of detection, limit of quantitation and limit of linearity 51
2.2.2.5 Construction of calibration curves 51
2.2.2.6 Validation 52
2.2.2.6 (a) Specificity 52
2.2.2.6 (b) Precision and accuracy 52
2.2.2.6 (c) Robustness 53
2.2.2.7 System suitability testing 53
2.3 Results 54
2.3.1 Limit of detection, limit of quantitation and limit of linearity 54

2.3.2 Calibration curve 55
2.3.3 Specificity 59
2.3.4 Precision and accuracy 60
2.3.5 Robustness 61
2.3.6 System suitability testing 68
2.4 Discussion 69
2.5 Conclusion 71

CHAPTER 3 - PREPARATION AND OPTIMIZATION OF PROCESS VARIABLES OF TYPE B GELATIN /CHITOSAN COMPLEX COACERVATION
3.1 Introduction 72
3.2 Materials and methods 73
3.2.1 Materials 73
3.2.2 Methods 74
3.2.2.1 Electrophoretic studies 74
3.2.2.2 Standard procedure for gelatin-chitosan complex coacervation 74
3.2.2.3 Observation of coacervate morphology 74
3.2.2.4 Degree of coacervation 75
3.2.2.5 Optimization of complex coacervation variables 75
3.2.2.5 (a) pH of coacervation 75
3.2.2.5 (b) Total polymer concentration and polymer mixing ratio 76
3.2.2.5 (c) Coacervation temperature 76
3.2.2.5 (d) Coacervation duration 77
3.2.2.5 (e) Incubation time 77
3.2.2.6 Coacervate droplet size 77
3.3 Results 78
3.3.1 Electrophoretic studies 78
3.3.2 pH of coacervation 79
3.3.3 Total polymer concentration and polymer mixing ratio 83
3.3.4 Coacervation temperature 91
3.3.5 Coacervation duration 92

3.3.6 Incubation time 94

3.4 Discussion 96

3.5 Conclusion 102

CHAPTER 4 - PREPARATION AND CHARACTERIZATION OF THE CURCUMINOIDS AND QUERCETIN MICROCAPSULES BY GELATIN B-CHITOSAN COMPLEX COACERVATION

4.1 Introduction 104

4.2 Materials and methods 106

4.2.1 Materials 106

4.2.2 Methods 106

4.2.2.1 Solubility of curcuminoids and quercetin in various mediums 106

4.2.2.2 Quantitation of curcuminoids and quercetin content in microcapsules 107

4.2.2.3 Complex coacervation microencapsulation and optimization – Investigation of curcuminoids and quercetin solid core microencapsulation 108

4.2.2.4 Curcuminoids/quercetin liquid core microencapsulation 110

4.2.2.5 Determination of microencapsulation efficiency 111

4.2.2.6 Physical characterization of microcapsules 112

4.2.2.6 (a) Microcapsule particle size 112

4.2.2.6 (b) Microcapsule wall thickness 112

4.2.2.6 (c) Morphology observation by optical microscope 112

4.2.2.6 (d) Morphology observation by SEM 112

4.2.2.6 (e) Colorimetric evaluation 113

4.2.2.6 (f) Appearance and staining testing 113

4.2.2.6 (g) Hygroscopicity 113

4.2.2.7 Physicochemical characterization 114

4.2.2.7 (a) Differential scanning calorimetry (DSC) 114

4.2.2.7 (b) Fourier transform infrared spectroscopy 114

4.2.2.8 Light stability 115

4.2.2.9 Storage stability 115

4.2.2.10 Swelling studies 116

4.2.2.11 Permeation study by using Franz diffusion cell 117

	4.2.2.12	Drug release kinetics study	119
	4.2.2.13	Determination of residual formaldehyde by gas chromatography	120
		4.2.2.13 (a) Chemicals and reagents	120
		4.2.2.13 (b) Instruments	121
	4.2.2.14	Statistical analysis	121
4.3	Results		122
	4.3.1	Solubility of curcuminoids and quercetin in various mediums	122
	4.3.2	Quantitation of curcuminoids and quercetin content in microcapsules	122
	4.3.3	Complex coacervation microencapsulation and optimization –Investigation of curcuminoids and quercetin solid core microcapsules	125
		4.3.3 (a) Influence of pH changing rate on microcapsule particle size and size distribution	125
		4.3.3 (b) Effect of drug concentration	127
		4.3.3 (c) Effect of microencapsulation equilibrium time	128
		4.3.3 (d) Effect of Tween 80 concentration	129
		4.3.3 (e) Effect of formaldehyde crosslinking	130
		4.3.3 (f) Effect of agitation rate	131
		4.3.3 (g) Effect of manner of agitation	134
	4.3.4	Curcuminoids/quercetin liquid core microencapsulation	136
	4.3.5	Physical characterization of microcapsules	136
		4.3.5 (a) Morphology, wall thickness and particle size	136
		4.3.5 (b) Morphology observation by SEM	141
		4.3.5 (c) Colorimetric evaluation	143
		4.3.5 (d) Appearance and staining testing	144
		4.3.5 (e) Hygroscopicity	147
	4.3.6	Physicochemical characterization of microcapsules	147
		4.3.6 (a) Differential scanning calorimetry (DSC)	147
		4.3.6 (b) Fourier transform infrared spectroscopy	152
	4.3.7	Light stability	161
	4.3.8	Storage stability	163
	4.3.9	Swelling studies	168
	4.3.10	Permeation studies by Franz diffusion cell	169

4.3.11 Drug release kinetics study 170
4.3.12 Determination of residual formaldehyde by gas chromatography 173
4.4 Discussion 174
4.5 Conclusion 185

CHAPTER 5 - FORMULATION AND CHARACTERIZATION OF MICROCAPSULE INCORPORATED CREAMS FOR TOPICAL APPLICATION
5.1 Introduction 186
5.2 Materials and methods 190
5.2.1 Materials 190
5.2.2 Methods 191
5.2.2.1 Construction of ternary phase diagram 191
5.2.2.1 (a) Fabrication of area of interest 191
5.2.2.1 (b) Fabrication of pseudo-ternary phase diagram and domain 192
5.2.2.2 Mixture design 192
5.2.2.3 Preparation of O/W creams and optimization of mixing methods 194
5.2.2.4 Cream characterization 195
5.2.2.4 (a) Organoleptic properties 195
5.2.2.4 (b) Cream type examination 195
5.2.2.4 (c) Microscopy observation 195
5.2.2.4 (d) Cream pH 196
5.2.2.4 (e) Zeta potential 196
5.2.2.4 (f) Particle size 196
5.2.2.4 (g) Rheological properties 197
5.2.2.4 (h) Texture analysis 198
5.2.2.5 Drug content 199
5.2.2.6 *In vitro* drug diffusion studies 199
5.2.2.7 Drug release kinetics studies 200
5.2.2.8 Stress testing 201
5.2.2.8 (a) Centrifugation test 201
5.2.2.8 (b) Freeze-thaw cycles test 201

	5.2.2.9	Storage stability	201
	5.2.2.10	Skin irritation test	202
	5.2.2.11	Statistical analysis	203
5.3	Results		204
	5.3.1	Construction of ternary phase diagram	204
		5.3.1 (a) Fabrication of area of interest	204
		5.3.1 (b) Fabrication of pseudo-ternary phase diagram and domain	205
	5.3.2	Mixture design	207
		5.3.2 (a) Mixture experimental design	207
		5.3.2 (b) Model establishment	211
		5.3.2 (c) Determination of the influence of design variables	214
		5.3.2 (d) Formulation optimization	218
	5.3.3	Preparation of O/W creams and optimization of mixing methods	219
	5.3.4	Cream characterization	223
		5.3.4 (a) Organoleptic properties	223
		5.3.4 (b) Cream type examination	224
		5.3.4 (c) Microscopy observation	224
		5.3.4 (d) Cream pH	225
		5.3.4 (e) Zeta potential	226
		5.3.4 (f) Particle size	227
		5.3.4 (g) Rheological properties	227
		5.3.4 (h) Texture analysis	229
	5.3.5	Drug content	230
	5.3.6	*In vitro* drug diffusion studies	232
	5.3.7	Drug release kinetics studies	233
	5.3.8	Stress testing	235
		5.3.8 (a) Centrifugation test	235
		5.3.8 (b) Freeze–thaw cycles test	235
	5.3.9	Storage stability	235
		5.3.9 (a) Organoleptic properties	235
		5.3.9 (b) Cream pH	235

5.3.9 (c) Zeta potential 237
5.3.9 (d) Particle size 238
5.3.9 (e) Rheological properties 241
5.3.9 (f) Texture analysis 242
5.3.9 (g) Drug content 243
5.3.10 Skin irritation test 248
5.4 Discussion 255
5.5 Conclusion 265

CHAPTER 6 - ANTIOXIDANT, ANTIBACTERIAL AND WOUND HEALING PROPERTIES OF CURCUMINOIDS AND QUERCETIN IN NATIVE AND MICROCAPSULE FORMS
6.1 Introduction 266
6.2 Materials and methods 268
6.2.1 Materials 268
6.2.2 Methods 269
6.2.2.1 Antioxidant activity 269
6.2.2.1 (a) Trolox equivalent antioxidant capacity (TEAC) 269
6.2.2.1 (b) Assessment of DPPH scavenging activity 270
6.2.2.2 Minimum inhibitory concentration 271
6.2.2.3 Effect of curcuminoids/quercetin and its encapsulated form on HaCaT cell 272
6.2.2.3 (a) Cell culture and treatments 272
6.2.2.3 (b) Cell cytotoxicity/viability determination by 3-(4,5-dimethylthiazol-2-yl)-2,5 diphenyltetrazolium bromide (MTT) assay 273
6.2.2.3 (c) Cell proliferation determination by 3-(4,5-dimethylthiazol-2-yl)-2,5 diphenyltetrazolium bromide (MTT) assay 273
6.2.2.3 (d) Cell migration determination by wound scratch assay 274
6.2.2.4 Effect of curcuminoids and quercetin microcapsule incorporated creams as controlled drug delivery on wound healing 274
6.2.2.4 (a) Animal models 275
6.2.2.4 (b) Burn wound 275
6.2.2.4 (c) Treatment 276

6.2.2.4 (d) Measurement of hydroxyproline 277
6.2.2.4 (e) Histopathologic study 277
6.2.2.5 Statistical analysis 278
6.3 Results 278
6.3.1 Antioxidant activity 278
6.3.1 (a) Trolox equivalent antioxidant capacity (TEAC) 278
6.3.1 (b) Assessment of DPPH scavenging activity 279
6.3.2 Minimum inhibitory concentration 280
6.3.3 Effect of curcuminoids/quercetin and its encapsulated form on HaCaT cell 281
6.3.3 (a) Cell cytotoxicity/viability determination by 3-(4,5-dimethylthiazol-2-yl)-2,5 diphenyltetrazolium bromide (MTT) assay 281
6.3.3 (b) Cell proliferation determination by 3-(4,5-dimethylthiazol-2-yl)-2,5 diphenyltetrazolium bromide (MTT) assay 283
6.3.3 (c) Cell migration determination by wound scratch assay 284
6.3.4 Effect of curcuminoids and quercetin microcapsule incorporated creams as controlled drug delivery on wound healing 285
6.3.4 (a) Wound contraction 285
6.3.4 (b) Measurement of hydroxyproline 292
6.3.4 (c) Histopathologic study 293
6.4 Discussion 295
6.5 Conclusion 302

CHAPTER 7 - SUMMARY AND CONCLUSION 304
CHAPTER 8 - SUGGESTIONS FOR FUTURE RESEARCH 307
REFERENCES 309
APPENDICES
LIST OF PUBLICATIONS

LIST OF TABLES

		Page
Table 1.1	A summary of surfactant HLB ranges and their applications	32
Table 1.2	Required hydrophilic-lipophilic balance (rHLB) for some oil-phase ingredients for oil-in-water (O/W) and water-in-oil (W/O) emulsions	34
Table 2.1	LOD, LOQ, LOL and linear regression analysis parameters for quercetin (QUE) and curcuminoids (BDMC, DMC and CUR)	54
Table 2.2	Retention times and responses data for calibration standards of quercetin (QUE) and curcuminoids (BDMC, DMC and CUR)	56
Table 2.3	Precision and accuracy for intraday and interday repetitions for the quantitative detection of quercetin (QUE) and curcuminoids (BDMC, DMC and CUR)	61
Table 2.4a	Robustness parameters: (a) Change in the organic composition by ± 2.0%	63
Table 2.4b	Robustness parameters: (b) Change in the acetic acid concentration by ± 1.0% v/v	64
Table 2.4c	Robustness parameters: (c) Change in the flow rate of ± 0.1 ml/min	65
Table 2.4d	Robustness parameters: (d) Change in the column temperature of ± 5.0 °C	66
Table 2.5	System suitability parameters, calculation formula and recommendations	68
Table 2.6	System suitability testing	69
Table 3.1	Coarcervate droplet size and size distribution at different total polymer concentrations and different mixing ratios for gelatin-chitosan systems	85
Table 3.2	Effect of reaction temperature on coarcervate droplet size and size distribution of gelatin-chitosan systems at total polymer concentration of 2.55% w/w and mixing ratio of 30:1	92
Table 3.3	Effect of coacervation duration on coarcervate droplet size and size distribution of the gelatin-chitosan systems at total polymer concentration of 2.55% w/w and mixing ratio of	94

30:1

Table 3.4 Effect of incubation time on coarcervate droplet size and size distribution of gelatin-chitosan systems at total polymer concentration of 2.55% w/w and mixing ratio of 30:1 95

Table 4.1 Solubility of curcumin and quercetin in various mediums 122

Table 4.2 Effect of disruption method on solubility of curcumin from curcuminoids microcapsule 123

Table 4.3 Particle size and size distribution influenced by pH adjustment rate using sodium hydroxide 125

Table 4.4 Effect of drug loaded amount on microencapsulation efficiency 128

Table 4.5 Effect of microencapsulation equilibrium time on microencapsulation efficiency 129

Table 4.6 Effect of Tween 80 concentration on microencapsulation efficiency 130

Table 4.7 Effect of formaldehyde concentration on microencapsulation efficiency 131

Table 4.8 Effect of formaldehyde crosslinking reaction time on microencapsulation efficiency 131

Table 4.9 Effect of agitation rate on microencapsulation efficiency 132

Table 4.10 Effect of agitation rate during microencapsulation on particle size and size distribution 133

Table 4.11 Effect of manner of agitation on microencapsulation efficiency for crosslinked- and uncrosslinked microcapsules 134

Table 4.12 The summary of optimized parameters for curcuminoids and quercetin solid core microencapsulation prepared by gelatin-chitosan complex coacervation (total polymer concentration was 2.55% w/w using gelatin:chitosan ratio of 30:1) 135

Table 4.13 Entrapment efficiency, drug loading and yield for CPM, QPM, CLM and QLM at optimized conditions 136

Table 4.14 Particle size and wall thickness for CPM, QPM, CLM and QLM 138

Table 4.15 Color space values for native drugs and microcapsules 143

Table 4.16	Hygroscopicity of microcapsules and native drug powders of curcuminoids and quercetin, samples stored at room temperature (28 ± 4 °C/75 ± 10% RH) for one week	147
Table 4.17	Rate equation reactant concentration-time profiles and half-lives for zero-, first-, and second order reactions	161
Table 4.18	Values of coefficient of determination (R2), rate constant (k) and half-life of degradation (t1/2) for curcuminoids, quercetin, CPM, CLM, QPM and QLM	162
Table 4.19	Exponent of the Korsmeyer-Peppas model and drug release mechanism for spherical geometry matrices	172
Table 4.20	Parameters of drug release kinetic models for native drug powders of curcuminoids and quercetin, and microcapsules of CPM and QPM	172
Table 5.1	Limits of the experimental domain	208
Table 5.2	Mixture design experiments and responses analyses for 2% curcuminoids microcapsule (CPM) incorporated creams with total required HLB of 10.325	209
Table 5.3	Mixture design experiments and responses analyses for 2% curcuminoids microcapsule (CPM) incorporated creams with total required HLB of 10.875	210
Table 5.4	Predicted response values with confidence interval (CI), prediction interval (PI) and standard errors (SE) analyzed by Design Expert® software DX6 for optimized cream formulation of oil phase:emulsifiers blend:aqueous phase = 30:12.95:57.05 (% w/w)	219
Table 5.5	Formulation of oil-in-water cream incorporated with 2% w/w curcuminoids (CPM)/quercetin (QPM) microcapsules	219
Table 5.6	Effect of mixing methods during emulsification on emulsion particle size and size distribution	220
Table 5.7	pH, particle size and zeta potential measurements of freshly prepared curcuminoids (CPM) and quercetin (QPM) creams	225
Table 5.8	Rheological properties of curcuminoids microcapsule (CPM) cream, quercetin microcapsule (QPM) cream and some marketed topical creams	228
Table 5.9	Firmness and work of shear values for curcuminoids microcapsule (CPM) cream, quercetin microcapsule (QPM) cream and some marketed topical creams	230

Table 5.10	Parameters of drug release kinetic models for curcuminoids microcapsule (CPM), quercetin microcapsule (QPM), CPM incorporated cream and QPM incorporated cream	234
Table 5.11	Ritger-Peppas diffusion exponent and mechanism of diffusional release from various swellable controlled release system	234
Table 5.12	Apparent viscosity and thixotropy of curcuminoids microcapsule (CPM) creams stored at 28 ± 4 °C/75 ± 10% RH and 40 ± 2 °C/75 ± 5% RH for 6 months; mean ± SD, n = 3	241
Table 5.13	Apparent viscosity and thixotropy of quercetin microcapsule (QPM) creams stored at 28 ± 4 °C/75 ± 10% RH and 40 ± 2 °C/75 ± 5% RH for 6 months; mean ± SD, n = 3	242
Table 5.14	Work of shear and firmness of curcuminoids microcapsule (CPM) creams stored at 28 ± 4 °C/75 ± 10% RH and 40 ± 2 °C/75 ± 5% RH for 6 months; mean ± SD, n = 3	242
Table 5.15	Work of shear and firmness of quercetin microcapsule (QPM) creams stored at 28 ± 4 °C/75 ± 10% RH and 40 ± 2 °C/75 ± 5% RH for 6 months; mean ± SD, n = 3	243
Table 5.16	Drug remaining (mg) and percent drug remaining (in bracket) of 2% w/w microcapsule (CPM/QPM) incorporated creams stored at 28 ± 4 °C/75 ± 10% RH and 40 ± 2 °C/75 ± 5% RH for 6 months	245
Table 5.17	Parameters of simple kinetic models for CPM cream and QPM cream stored at room temperature (28 ± 4 °C/75 ± 10% RH) and elevated temperature (40 ± 2 °C/75 ± 5% RH) for 6 months	245
Table 5.18	Grading of skin reactions	248
Table 6.1	Antioxidant activity of curcuminoids and quercetin (both in native and microcapsule forms), BHA and BHT	279
Table 6.2	Minimum inhibitory concentrations of curcuminoids and quercetin (both in native and microcapsule forms) and antibiotics of gram positive and gram negative bacteria	280

LIST OF FIGURES

		Page
Figure 1.1	Chemical structures of curcumin, demethoxycurcumin and bisdemethoxycurcumin	3
Figure 1.2	Chemical structure of quercetin	5
Figure 1.3	Schematic morphologies of different types of microcapsules: (A) matrix, (B) single structure microcapsule (regular), (C) irregular single structure microcapsule, (D) multiwall microcapsule, (E) multi-core microcapsule and (F) aggregate structure microcapsule	8
Figure 1.4	Chemical structure of gelatin	13
Figure 1.5	Chemical structure of chitosan	14
Figure 1.6	Formation of methylene glycol and formaldehyde polymer	17
Figure 1.7	Formaldehyde crosslinking: formation of methylene glycol and methylene bridge	18
Figure 1.8	Schematic morphologies of (a) microcapsule and (b) microsphere	19
Figure 1.9	Process of microencapsulation by complex coacervation: (a) emulsification or suspension of core ingredients in the vehicle phase (typically aqueous solution); (b) induce complex coacervation by addition of a second complexing hydrocolloid; (c) solidification of wall materials and crosslink to stabilize the microcapsules; and (d) washing and drying	23
Figure 1.10	Schematic representation of microencapsulation by coacervation: (a) dispersed liquid or solid drug particles, (b) induction of phase separation, (c) deposition of microdroplets at the surface, and (d) fusion into a membrane	24
Figure 1.11	Drug release mechanisms from microcapsules: (a) diffusion, (b) dissolution, (c) osmosis, and (d) erosion	27
Figure 1.12	Common breadown processes of emulsions	40
Figure 2.1	Chemical structures of quercetin, bisdemethoxycurcumin, demethoxycurcumin and curcumin	47
Figure 2.2	Quercetin calibration curve	57

Figure 2.3	Bisdemethoxycurcumin calibration curve	57
Figure 2.4	Demethoxycurcumin calibration curve	58
Figure 2.5	Curcumin calibration curve	58
Figure 2.6	Chromatogram of QUE, quercetin; BDMC, bisdemethoxycurcumin; DMC, demethoxycurcumin; and CUR, curcumin	59
Figure 2.7	Chromatograms of (a) methanol, (b) ethanol, (c) mobile phase, (d) citrate-phosphate buffer pH 5.4, (e) cream base and (f) gelatin-chitosan coacervate microcapsule	60
Figure 2.8	Combined chromatograms of quercetin (QUE), bisdemethoxycurcumin (BDMC), demethoxycurcumin (DMC) and curcumin (CUR) analyzed at different conditions: (a) change in the organic composition by ± 2%; (b) change in the acetic acid concentration by ± 1.0% v/v; (c) change in the flow rate of mobile phase of ± 0.1 ml/min; and (d) change in the column temperature of ± 5.0 °C	67
Figure 3.1	Zeta potential measurements as a function of pH: (a) chitosan solution (0.04% w/w), and (b) type B gelatin solution (1% w/w) with ionic strength of 0.1 M NaCl, performed at 25 °C. Mean ± SD, n = 3	79
Figure 3.2	Effect of pH on turbidity index and dry coacervate yield of gelatin-chitosan systems at total polymer concentration of 2.55% w/w and mixing ratio of 30:1. The process was carried out by constant stirring at 500 rpm for 0.5 h, at 50 °C. Mean ± SD, n = 3	81
Figure 3.3	Effect of total polymer concentration and gelatin-chitosan mixing ratio on turbidity index. Coacervations were induced at pH 5.50 with constant stirring for 0.5 h, at 50 °C. Mean ± SD, n = 3	88
Figure 3.4	Dry coacervate yields obtained from gelatin-chitosan systems at different total polymer concentrations and different mixing ratios. Coacervations were induced at pH 5.50 with constant stirring at 500 rpm for 0.5 h, at 50 °C. Mean ± SD, n = 3	90
Figure 3.5	Different coacervate volumes and dry coacervate yields obtained from gelatin-chitosan systems at ratio of 30:1, of different total polymer concentrations. Coacervations were induced at pH 5.50 with constant stirring at 500 rpm for 0.5 h, at 50 °C Mean ± SD, n = 3	90

Figure 3.6	Effect of coacervation temperature on turbidity index and dry coacervate yield of gelatin-chitosan systems at total polymer concentration of 2.55% w/w and mixing ratio of 30:1. Coacervations were induced at pH 5.50 with constant stirring at 500 rpm for 0.5 h. Mean ± SD, n = 3	91
Figure 3.7	Effect of coacervation duration of the gelatin-chitosan systems at total polymer concentration of 2.55% w/w and mixing ratio of 30:1 on colloids turbidity index and dry coacervate yield. The pH and temperature of coacervation were 5.50 and 50 °C, respectively. Mean ± SD, n = 3	93
Figure 3.8	Effect of incubation time of gelatin-chitosan systems at total polymer concentration of 2.55% w/w and mixing ratio of 30:1 on turbidity index and dry coacervate yield. The coacervations were induced at pH 5.50 with constant stirring at 500 rpm for 0.5 h, at 50 °C. Mean ± SD, n = 3	95
Figure 4.1	Schematic diagram for the preparation of gelatin-chitosan coacervation microcapsules containing solid or liquid core materials	111
Figure 4.2	The static Franz cell and the experimental setup using #V3 3-Station Franz Cell Stirrer	118
Figure 4.3	HPLC chromatograms of (a) CPM, curcuminoids solid core microcapsule; (b) CLM, curcuminoids liquid core microcapsule; (c) QPM, quercetin solid core microcapsule and (d) QLM, quercetin liquid core microcapsule	124
Figure 4.4	Effect of pH changing rate on particle size distribution for curcuminoids solid core microcapsules: (a) 25 µl/10 sec and (b) 200 µl/10 sec	126
Figure 4.5	DSC thermograms of raw material powders: gelatin, chitosan, curcuminoids and quercetin	148
Figure 4.6	DSC thermograms of crosslinked CPM, uncrosslinked CPM, crosslinked CLM, blank microcapsule and physical mixtures of raw materials	151
Figure 4.7	DSC thermograms of crosslinked QPM, uncrosslinked QPM, crosslinked QLM, blank microcapsule and physical mixtures of raw materials	151
Figure 4.8	FTIR spectra of gelatin, chitosan and blank microcapsule	154
Figure 4.9	FTIR spectra of native curcuminoids and quercetin powders	155
Figure 4.10	FTIR spectra of blank microcapsule, CPM and CLM	158

Figure 4.11	FTIR spectra of blank microcapsule, QPM and QLM	159
Figure 4.12	FTIR overlay spectra of CPM and CLM	160
Figure 4.13	FTIR overlay spectra of QPM and QLM	160
Figure 4.14	Zero order kinetics plots of light stability data for native curcuminoids, CPM and CLM. Data points are mean value of triplicate measurements	162
Figure 4.15	First order kinetics plots of light stability data for native curcuminoids, CPM and CLM. Data points are mean value of triplicate measurements	163
Figure 4.16	Drug retention of native curcuminoids, native quercetin, CPM, QPM, CLM and QLM stored at 28 ± 4 °C/75 ± 10% RH for 12 months. ** and *** indicate significant difference at $p < 0.01$ and at $p < 0.001$, respectively compared to control. Mean ± SD, n = 3	164
Figure 4.17	Drug retention of native curcuminoids, native quercetin, CPM, QPM, CLM and QLM stored at 40 ± 2 °C/75 ± 5% RH for 6 months. *** indicates significant difference at $p < 0.001$ compared to control. Mean ± SD, n = 3	165
Figure 4.18	Drug retention of native curcuminoids, native quercetin, CPM, QPM, CLM and QLM stored at 5 ± 3 °C for 6 months. ** and *** indicate significant difference at $p < 0.01$ and at $p < 0.001$, respectively compared to control. Mean ± SD, n = 3	165
Figure 4.19	Particle size of CPM, QPM, CLM and QLM stored at 28 ± 4 °C/75 ± 10% RH for 12 months. *** indicates significant difference at $p < 0.001$ compared to control. Mean ± SD, n = 3	166
Figure 4.20	Particle size of CPM, QPM, CLM and QLM stored at 40 ± 2 °C/75 ± 5% RH for 6 months. ** and *** indicate significant difference at $p < 0.01$ and at $p < 0.001$, respectively compared to control. Mean ± SD, n = 3	167
Figure 4.21	Particle size of CPM, QPM, CLM and QLM stored at 5 ± 3 °C for 6 months. Mean ± SD, n = 3	167
Figure 4.22	Comparison of swelling index for various microcapsules in different media at 35 ± 2 °C. Mean ± SD, n = 3	168
Figure 4.23	Release profiles of native curcuminoids, crosslinked CPM and uncrosslinked CPM	169

Figure 4.24	Release profiles of native quercetin, crosslinked QPM and uncrosslinked QPM	170
Figure 4.25	Chromatograms of formaldehyde analysis by gas chromatography: (a) internal standard solution (1-butanol), (b) standard solution containing 0.1% formaldehyde and 1-butanol, (c) crosslinked CPM and (d) crosslinked QPM	173
Figure 5.1	The set-up of TTC Spreadability fixture on the Heavy Duty Platform	199
Figure 5.2	Pseudo-ternary phase diagram of oil, water and emulsifiers blend showing oil-in-water region	205
Figure 5.3	Combination points in area of interest of ternary phase diagram and the oil-in-water cream formulations (highlighted area)	206
Figure 5.4	Construction of pseudo ternary phase diagram (L-transformation) and parallelogram (domain)	207
Figure 5.5	The normal probability plots for experimental responses: (a) apparent viscosity, (b) firmness and (c) work of shear	212
Figure 5.6	The predicted versus actual plots for experimental responses: (a) apparent viscosity, (b) firmness and (c) work of shear	213
Figure 5.7	Response trace plots of (a) apparent viscosity, (b) firmness and (c) work of shear. A: oil components = 29.97%, B: emulsifiers blend = 12.97%, C: aqueous phase = 56.91%	215
Figure 5.8	3D surface plots: (a) apparent viscosity, (b) firmness and (c) work of shear. X1: oil phase, X2: emulsifier blend and X3: aqueous phase	217
Figure 5.9	Size distribution graphs of cream bases emulsified by: (a) mechanical mixing at 2000 rpm for 15 min, (b) mechanical mixing and homogenization at 18000 rpm for 2 min and (c) mechanical mixing and homogenization at 18000 rpm for 2 min, 3 cycles	221
Figure 5.10	Zeta potential charge distribution of curcuminoids microcapsule (CPM) cream (n = 3)	226
Figure 5.11	Zeta potential charge distribution of quercetin microcapsule (QPM) cream (n = 3)	226
Figure 5.12	Rheograms of (a) curcuminoids microcapsule (CPM) cream and (b) quercetin microcapsule (QPM) cream	229

Figure 5.13	HPLC chromatograms of (a) curcuminoids microcapsule (CPM) cream and (b) quercetin microcapsule (QPM) cream	231
Figure 5.14	*In vitro* drug release profiles of crosslinked curcuminoids microcapsule (CPM), crosslinked quercetin microcapsule (QPM), CPM cream and QPM cream	232
Figure 5.15	pH values of CPM and QPM creams stored at 28 ± 4 °C/75 ± 10% RH and 40 ± 2 °C/75 ± 5% RH for 6 months; mean ± SD, n = 3. * represents significant difference compared to control at $p < 0.05$	236
Figure 5.16	Zeta potential values of CPM cream stored at 28 ± 4 °C/75 ± 10% RH and 40 ± 2 °C/75 ± 5% RH for 6 months; mean ± SD, n = 3	237
Figure 5.17	Zeta potential values of QPM cream stored at 28 ± 4 °C/75 ± 10% RH and 40 ± 2 °C/75 ± 5% RH for 6 months; mean ± SD, n = 3. * represents significant difference compared to control at $p < 0.05$	238
Figure 5.18	Particle size and span values of CPM cream stored at 28 ± 4 °C/75 ± 10% RH and 40 ± 2 °C/75 ± 5% RH for 6 months; mean ± SD, n = 3. * represents significant difference compared to control at $p < 0.05$	239
Figure 5.19	Particle size and span values of QPM cream stored at 28 ± 4 °C/75 ± 10% RH and 40 ± 2 °C/75 ± 5% RH for 6 months; mean ± SD, n = 3. * represents significant difference compared to control at $p < 0.05$	239
Figure 5.20	Size distribution of creams containing 2% w/w curcuminoids microcapsule (a-c) and 2% w/w quercetin microcapsule (d-f). Graphs (a) and (d) represented freshly prepared creams; graphs (b) and (e), (c) and (f) represented creams stored at 28 ± 4 °C/75 ± 10% RH and 40 ± 2 °C/75 ± 5% RH, respectively for 6 months	240
Figure 5.21	Simple order kinetic plots of drug degradation data for curcuminoids microcapsule (CPM) creams	246
Figure 5.22	Simple order kinetic plots of drug degradation data for quercetin microcapsule (QPM) creams	247
Figure 6.1	A modified stainless steel stamp (20 mm in diameter) with an electronic temperature controller	276
Figure 6.2	Effect of native curcuminoids, native quercetin, curcuminoids microcapsule (CPM) and quercetin microcapsule (QPM) at various concentrations on HaCaT	282

cell viability. Results were expressed as mean ± SD of three independent tests. * indicates $p < 0.05$ compared to the untreated control

Figure 6.3 Effect of native curcuminoids, native quercetin, curcuminoids microcapsule (CPM) and quercetin microcapsule (QPM) on HaCaT cell proliferation. Each point represents the mean of three independent tests 283

Figure 6.4 Effect of native curcuminoids, native quercetin, curcuminoids microcapsule (CPM) and quercetin microcapsule (QPM) on scratch wound repair of HaCaT cells. Results were expressed as mean ± SD of three independent tests 285

Figure 6.5 Effect of cream base, Silfazine cream (positive control), CPM cream and QPM cream on wound contraction compared to normal saline negative control group (n = 6). Results were expressed as mean ± S.E.M. * and ** indicate significant difference at $p < 0.05$ and $p < 0.01$, respectively compared to normal saline treated group 286

Figure 6.6 Effect of cream base, Silfazine cream (positive control), CPM cream and QPM cream on hydroxyproline content in wound tissue compared to normal saline negative control group (n = 6). Results were expressed as mean ± S.E.M. * and ** indicate significant level at $p < 0.05$ and $p < 0.01$, respectively compared to normal saline treated group 292

LIST OF PLATES

		Page
Plate 3.1	Micrographs show the coacervation of the gelatin-chitosan system at total polymer concentration of 2.55% w/w and mixing ratio of 30:1, with different pH values: (a) pH 4.75, (b) pH 5.00, (c) pH 5.25, (d) pH 5.50, (e) pH 5.75, and (f) pH 6.00. Bar represents 20 µm	82
Plate 3.2	Coacervation and precipitation systems obtained from gelatin-chitosan colloids at 2.55% w/w of different mixing ratios induced at pH 5.50	83
Plate 3.3	Micrographs show the gelatin-chitosan systems at total polymer concentration of 2.55% w/w with different ratios: (a) 10:1, (b) 15:1, (c) 20:1, (d) 25:1, (e) 30:1, (f) 35:1, (g) 40:1, (h) 50:1, (i) 60:1, and (j) 80:1. Bar represents 20 µm	86
Plate 3.4	Micrographs show the gelatin-chitosan systems at ratio 30:1, with different total polymer concentrations: (a) 1.55, (b) 2.05, (c) 2.55, (d) 3.05, and (e) 3.55% w/w. Bar represents 20 µm	87
Plate 3.5	The physical appearance of the gelatinized gelatin-chitosan colloids at total polymer concentration of 2.55% w/w and mixing ratios from 10:1 to 80:1.	88
Plate 3.6	The physical appearance of the gelatin-chitosan systems at total polymer concentration of 2.55% w/w and mixing ratio of 30:1 equilibrated at different coacervation durations	93
Plate 4.1	Micrographs show the curcuminoids solid core microcapsules' configuration by the effect of pH changing rate: (a) 25 µl/10 sec, (b) 50 µl/10 sec, (c) 100 µl/10 sec and (d) 200 µl/10 sec. Bars represent 10 µm	126
Plate 4.2	Micrographs show the effect of agitation rate during microencapsulation on configuration of curcuminoids solid core microcapsules: (a) 400 rpm, (b) 500 rpm, (c) 600 rpm and (d) 700 rpm. Bars represent 10 µm	133
Plate 4.3	Micrographs show the morphologies of (a) curcuminoids powder and (b) quercetin powder. Bar represents 20 µm	137
Plate 4.4	Micrographs show the configurations of microcapsules: (a) CLM, curcuminoids liquid core microcapsule; (b) QLM, quercetin liquid core microcapsule; (c) CPM, curcuminoids solid core microcapsule (d) QPM, quercetin solid core microcapsule (e) aggregate CPM, and (f) aggregate QPM. Bars represent 5 µm (a & b), 2 µm (c & d) and 1 µm (e & f),	139

respectively

Plate 4.5 Micrographs show the double layer of capsule wall in (a): CLM, curcuminoids liquid core microcapsule and (b): single layer of capsule wall in CPM, curcuminoids solid core microcapsule 140

Plate 4.6 SEMs for (a) crosslinked CPM and (b) uncrosslinked CPM 142

Plate 4.7 Pictures show the physical appearance and the staining effect of: (a) native curcuminoids powder, (b) curcuminoids solid core microcapsule powder, CPM and (c) curcuminoids liquid core microcapsule powder, CLM 145

Plate 4.8 Pictures show the physical appearance and the staining effect of: (a) native quercetin powder, (b) quercetin solid core microcapsule powder, QPM and (c) quercetin liquid core microcapsule powder, QLM 146

Plate 5.1 Micrographs show the emulsion droplet configurations produced by (a) mechanical mixing at 2000 rpm for 15 min, (b) mechanical mixing and homogenization at 18000 rpm for 2 min, and (c) mechanical mixing and homogenization at 18000 rpm for 2 min, 3 cycles. Bars represent 50 μm 222

Plate 5.2 Photos show the physical appearance of cream base, quercetin microcapsule (QPM) cream and curcuminoids microcapsule (CPM) cream 223

Plate 5.3 Methylene blue being dissolved and homogeneously diffused throughout the external phase of the O/W cream 225

Plate 5.4 Micrographs of (a) curcuminoids microcapsule (CPM) cream and (b) quercetin microcapsule (QPM) cream. Bars represent 5 μm 225

Plate 5.5 Skin irritation test of curcuminoids microcapsule (CPM) cream – evidence and grading 249

Plate 5.6 Skin irritation test of quercetin microcapsule (QPM) cream – evidence and grading 252

Plate 6.1 Photographs of macroscopic appearance of wound contraction treated with normal saline at day 1 (a), day 3 (b), day 6 (c), day 9 (d), day 12 (e), day 15 (f), day 18 (g) and day 21 (h) 287

Plate 6.2 Photographs of macroscopic appearance of wound contraction treated with cream base 0.5 g/day at day 1 (a), day 3 (b), day 6 (c), day 9 (d), day 12 (e), day 15 (f), day 18 288

(g) and day 21 (h)

Plate 6.3 Photographs of macroscopic appearance of wound contraction treated with Silfazine cream 0.5 g/day at day 1 (a), day 3 (b), day 6 (c), day 9 (d), day 12 (e), day 15 (f), day 18 (g) and day 21 (h) 289

Plate 6.4 Photographs of macroscopic appearance of wound contraction treated with CPM cream 0.5 g/day at day 1 (a), day 3 (b), day 6 (c), day 9 (d), day 12 (e), day 15 (f), day 18 (g) and day 21 (h) 290

Plate 6.5 Photographs of macroscopic appearance of wound contraction treated with QPM cream 0.5 g/day at day 1 (a), day 3 (b), day 6 (c), day 9 (d), day 12 (e), day 15 (f), day 18 (g) and day 21 (h) 291

Plate 6.6 Hematoxylin and Eosin stained section of skin burn wound from: (a) normal saline (negative control), (b) cream base-treated, (c) Silfazine cream-treated, (d) CPM cream-treated and (e) QPM cream-treated groups; (E) Epidermis, (S) scab, (D) dermis, (EGT) early granulation tissue, (GT) granulation tissue, (star) aggregation of inflammatory cells, (R) rete ridges and (→) epithelialization 294

LIST OF ABBREVIATIONS

%T	transmittance percent
$\dot{\gamma}$	Shear rate
τ_0	Yield stress
<	Less than
>	More than
±	Plus minus
µg/ml	Microgram per millimeter
µl	Microliter
µm	Micrometer
ABTS	2,2'-azino-*bis* (3-ehylbenzothiazoline-6-sulfonate)
BDMC	Bisdemethoxycurcumin
BHA	Butylated hydroxyanisole
BHT	Butylated hydroxytoluene
CLM	Curcuminoid microcapsule (liquid core microencapsulation)
cm	Centimeter
$-COO^-$	Carboxylate
-COOH	Carboxyl group
CPM	Curcuminoid microcapsule (solid core microencapsulation)
CUR	Curcumin
D[4,3]	Volume mean diameter
DMC	Demethoxycurcumin
DPPH	2,2-diphenyl-1-picrylhydrazyl
DSC	Differential scanning calorimetry
FTIR	Fourier transform infrared spectroscopy
HCl	Hydrochloric acid
HLB	Hydrophilic-lipophilic balance
IP	Intraperitoneal injection
K	Release rate constant or consistency coefficient
k'	Capacity factor
LOD	Limit of detection
LOL	Limit of linearity
LOQ	Limit of quantitation
M	Molar
min	Minute
ml	Milliliter
ml/min	Milliliter per minute
mm	Millimeter
N	Theoretical plate
n	Flow behavior index or release exponent
Ŋ	Apparent viscosity
N_2	Gas nitrogen
NaCl	Sodium chloride
ng/ml	Nanogram per millimeter
$-NH_2$	Amino group
$-NH_3^+$	Ammonium
nm	Nanometer
O/W	Oil-in-water

pH_c	Critical pH
pH_ϕ	pH of macroscopic/global phase separation,
pI	Isoelectric point
QC	Quality control
QLM	Quercetin microcapsule (liquid core microencapsulation)
QPM	Quercetin microcapsule (solid core microencapsulation)
QUE	Quercetin
R	Resolution
R^2	Coefficient of determination
RH	Relative humidity
rHLB	Hydrophilic-lipophilic balance requirement
RP-HPLC	Reversed phase high performance liquid chromatography
rpm	Rotation per minute
RSD	Relative standard deviation
S.E.M	Standard error of mean
S/N	Signal to noise
SD	Standard deviation
SEM	Scanning electron microscope
Smix	Emulsifiers blend
$t_{1/2}$	Half-life of degradation
$t_{50\%}$	Half-life of release
t_{90}	Shelf life or time of 10% decomposition
T_f	Tailing factor
t_R	Retention time
UV	Ultraviolet
v/v	Volume per volume
W/O	Water-in-oil
w/w	Weight per weight
μM	Micro molar
τ	Shear stress

LIST OF APPENDICES

Appendix A1	Chromatograms of quercetin (10 μg/ml) and curcuminoids (100 μg/ml)
Appendix B1	Formulation and method of preparation of type B gelatin-chitosan mixture solution at different ratios and total polymer concentrations
Appendix C1	Preparation of citrate-phosphate buffer
Appendix C2	Preparation of citrate buffer
Appendix D1	Calculation of required hydrophile-lipophile balance (rHLB) of oil phase ingredients
Appendix D2	Calculation for relative quantities of emulsifying agents necessary to produce the physically stable emulsion
Appendix E1	The drawing of straight lines from the middle of each apex to the opposite apex and the location of 27 screening points for fabrication of ternary phase diagram
Appendix E2	Screening points and types of combination
Appendix E3	Combination points constructed in the area of interest
Appendix F1	Statistical analyses for apparent viscosity, firmness and work of shear
Appendix G1	Approval letter for use of rabbits for primary skin irritation test
Appendix G2	Approval letter for use of rats for wound healing study

MIKROKAPSUL KOASERVAT KOMPLEKS DALAM KRIM UNTUK PENGHANTARAN TOPIKAL KURKUMINOID DAN QUERCETIN

ABSTRAK

Kurkuminoid dan quercetin mempunyai aktiviti antioksidan, anti-radang dan anti-bakteria yang bermanfaat untuk penyembuhan luka. Walau bagaimanapun, sifat kedua-dua sebatian ini iaitu kelarutan dan bio-keperolehan yang rendah, fotosensitiviti dan pewarnaan menjadikan sebatian-sebation tersebut kurang sesuai untuk pemakaian topical. Oleh itu, objektif kajian ini adalah untuk membangunkan dan mencirikan mikrokapsul kurkuminoid dan quercetin, dan seterusnya menggabungkan sebatian-sebatian ini ke dalam krim. HPLC UV fasa terbalik isokratik dibangunkan dan disahkan untuk menyatakan kuantiti kurkuminoid (bisdemethoxycurcumin, demethoxycurcumin dan curcumin) dan quercetin secara serentak. Puncak quercetin, bisdemethoxycurcumin, demethoxycurcumin dan curcumin adalah terpisah dan simetri. Mikrokapsul telah disediakan dengan menggunakan kaedah koaservation kompleks menggunakan chitosan dan gelatin B. Mikrokapsul terbaik diperolehi dengan gelatin:chitosan pada nisbah 30:1 (2.55% w/w) dan pH 5.50. Kurkuminoid dikapsulkan sama ada dalam bentuk cecair (CLM) atau pepejal (CPM). Quercetin juga dikapsulkan sama ada dalam bentuk cecair (QLM) atau pepejal (QPM). Ciri-ciri fizikal bagi CPM dan QPM adalah lebih baik daripada CLM dan QLM. CPM dan QPM mempunyai saiz zarah dalam linkungan 40-44 μm, kecekapan pemerangkapan sebanyak 82% dan memuatkan ubat 16%. Selain itu, mikrokapsul ini tidak melekit, kurang kesan pewarnaan dan stabil pada suhu bilik (28 °C) selama 12 bulan. Aktiviti antioksidan kurkuminoid dan quercetin adalah lebih tinggi daripada hidroksianisol dibutilkan (BHA) dan hidroksitoluena

dibutilkan (BHT). Tiada perubahan ketara dalam aktiviti antioksidan kurkuminoid dan quercetin selepas pengkapsulan dalam mikrokapsul. Kurkuminoid dan quercetin kemudiannya masing-masing digabungkan ke dalam asas krim O/W. Kedua-dua sediaan ini mempunyai ciri-ciri pseudoplastik dan tiksotropik. Kajian pelepasan *in vitro* menunjukkan bahawa kurkuminoid dan quercetin dilepaskan dari mikrokapsul yang digabungkan di dalam krim mengikuti kinetic tertib sifar. Krim-krim CPM dan QPM stabil pada suhu bilik (28 °C) selama 6 bulan. Ujian kerengsaan kulit pada arnab menunjukkan bahawa kedua-dua sediaan tidak merengsa. Tambahan pula, kajian *in vivo* penyembuhan luka pada tikus menunjukkan bahawa krim CPM dan krim QPM mempunyai sifat penyembuhan luka. Kesimpulannya, mikrokapsul kurkuminoid dan quercetin yang digabungkan dalam krim telah berjaya disediakan. CPM mempunyai ciri-ciri penyembuhan luka yang lebih baik daripada QPM.

COMPLEX COACERVATED MICROCAPSULES IN CREAM FOR TOPICAL DELIVERY OF THE CURCUMINOIDS AND QUERCETIN

ABSTRACT

The curcuminoids and quercetin possess antioxidant, anti-inflammatory and antibacterial activities which are beneficial for wound healing. However, poor solubility, poor bioavailability, photosensitivity and color staining properties of these two compounds make them not acceptable for topical administrations. Therefore, the objectives of the present study were to develop and characterize the curcuminoids/quercetin microcapsules and subsequently incorporate them in cream. Isocratic reversed phase UV HPLC was developed and validated to quantify the curcuminoids (bisdemethoxycurcumin, demethoxycurcumin and curcumin) and quercetin simultaneously. The peaks of quercetin, bisdemethoxycurcumin, demethoxycurcumin and curcumin were well separated and symmetrical. The microcapsules were prepared by complex coacervation method using chitosan and gelatin B. The best microcapsules were obtained at gelatin:chitosan ratio of 30:1 (2.55% w/w) and pH 5.50. The curcuminoids was encapsulated either in liquid (CLM) or solid (CPM) form. The quercetin was also encapsulated either in liquid (QLM) or solid (QPM) form. The physical characteristics of CPM and QPM were better than CLM and QLM. The CPM and QPM had particle size in the range of 40 – 44 μm, entrapment efficiency of 82% and drug loading of 16%. Moreover, the microcapsules had free flowing, reduce color staining effect and stable at room temperature (28 °C) for 12 months. The antioxidant activity of the curcuminoids and quercetin was higher than butylated hydroxyanisole (BHA) and butylated hydroxytoluene (BHT). There was no significant change in antioxidant activity of the

curcuminoids and quercetin after encapsulation in microcapsules. The curcuminoids and quercetin microcapsules were then incorporated in O/W cream base, respectively. The preparations had pseudoplastic and thixotropic properties. *In vitro* release study revealed that the curcuminoids and quercetin released from microcapsule incorporated in cream followed zero order kinetics. The CPM and QPM creams were stable at room temperature (28 °C) for 6 months. The skin irritation test in rabbit revealed that both preparations were nonirritant. Furthermore, the *in vivo* wound healing study in rats showed that CPM and QPM creams had wound healing properties. In conclusion, the curcuminoids and quercetin microcapsules incorporated in creams were successfully prepared. CPM had better wound healing property than QPM.

CHAPTER 1

INTRODUCTION

1.1 Active ingredients

1.1.1 Curcuminoids/curcumin

The turmeric plant is a herb belonging to *Curcuma longa* L. (Zingiberaceae family) and has been widely used for centuries as a dietary spice and coloring agent in Indian and Chinese cuisines. The dried ground rhizome of the plant has been used in Asian medicine since the second millennium BC. Extracts of the rhizome including turmerin (a water-soluble peptide), essential oil (e.g., turmerones, atlantones and zingiberene) and curcuminoids [consists of curcumin (~77%), demethoxycurcumin (~17%), bisdemethoxycurcumin (~3%) and cyclocurcumin] (Akbik et al., 2014; Maheshwari et al., 2006; Naksuriya et al., 2014; Prasad et al., 2014; Sharma et al., 2005).

The three major analogues of the curcuminoids namely, curcumin, demethoxycurcumin (DMC) and bisdemethoxycurcumin (BDMC) differ by a methoxy substitution on the aromatic ring (Figure 1.1). Curcumin has two symmetric *o*-methoxy phenols linked through the α,β-unsaturated β-diketone moiety, DMC has an asymmetric structure with one of the phenyl rings having *o*-methoxy substitution, and BDMC is similar to curcumin with its symmetric structure but is deficient in two *o*-methoxy substitutions. These analogues have different potential in terms of bioactivities (Anand et al., 2008).

Curcumin as the major component of curcuminoids is responsible for the yellow color that consists of 3-6% of turmeric preparations. Curcumin was discovered about two centuries ago by Vogel and Pelletier in the year 1815 (cited by Prasad et al., 2014). In year 1910, the chemical structure of curcumin [i.e., diferulyoylmethane or 1,7-bis (4-hydroxy-3-methoxy-phenyl) hepta-1,6-diene-3,5-dione), $C_{21}H_{20}O_6$] was reported by Milobedzka et al. (1910), as cited in Prasad et al. (2014). The first synthesis and chromatographic quantitation of curcumin were reported in years 1913 and 1953, respectively. Curcumin is practically insoluble in water at acidic and neutral pH but is soluble in methanol, ethanol, dimethylsulfoxide, and acetone. It has pKa value of 8.54 (Prasad et al., 2014). Curcumin exist in two molecular configurations that are, bis-keto and enolate. The keto form predominates in acidic and neutral conditions and in the solid phase, where curcumin acts as a potent donor of hydrogen atoms. The enol form consists of three ionizable protons corresponding to the enolic group and two phenolic groups, which predominate in alkaline conditions. However, curcumin is photosensitive and unstable in phosphate buffer systems of pH 7.2 (Goel et al., 2008; Strimpakos & Sharma, 2008; Wang et al., 1997).

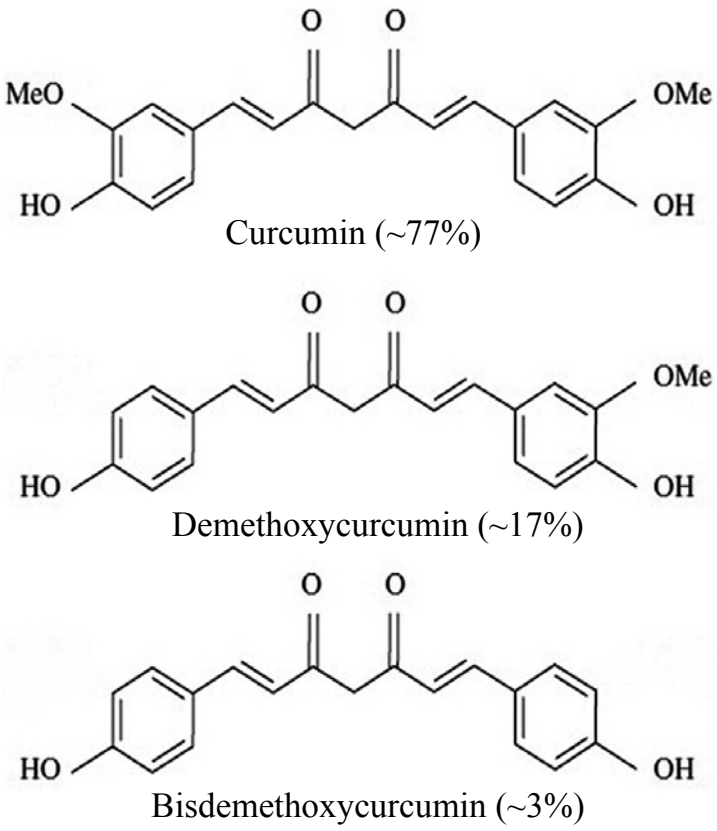

Figure 1.1. Chemical structures of curcumin, demethoxycurcumin and bisdemethoxycurcumin.

The biological characteristics of curcumin derivatives (demethoxycurcumin and bisdemethoxycurcumin) and curcumin were scientifically investigated in the mid-twentieth century (Prasad et al., 2014). Curcumin and derivatives of curcumin are typical flavonoid compounds, exhibit a wide range of pharmacological activities, such as anti-cancer (Anto et al., 1996; Ruby et al., 1995; Panahi et al., 2014), antioxidant (Jayaprakasha et al., 2006), anti-angiogenic (Gururaj et al, 2002; Kant et al., 2015), antibacterial (Sivasothy et al., 2013), anti-inflammatory (Kant et al., 2014), antiviral and antifungal (Anand et al., 2008). Curcumin is also a multidrug resistance modulator (Xue et al., 2013). Additionally, the curcuminoids have been shown to

have medicinal properties against several acute and chronic diseases including type II diabetes, rheumatoid arthritis, multiple sclerosis, Alzheimer's disease, Parkinson's disease, cardiovascular diseases, allergies, atherosclerosis and certain types of cancer (Li & Zhang, 2014; Maheshwari et al., 2006; Srivastava et al., 2011; Villaflores et al., 2012). Curcuminoids have been explored in enhancement of wound healing, hepatoprotection, treatment of inflammatory disease, neoplastic disease, neurodegenerative disease, cystic fibrosis and cholesterol-lowering (Akbik et al., 2014; Cao et al., 2015; Castangia et al., 2014; Kant et al., 2014).

In vivo studies show the safety of curcumin following acute and subchronic administration to rats and mice. High doses of dietary curcumin show no adverse effects in humans and animals (Sharma et al., 2005).

1.1.2 Quercetin

Quercetin is a flavonol compound belonging to a broad group of polyphenolic flavonoids. Quercetin is present in food as quercetin glycosides which represent 60-75% of the total dietary flavonols plus flavones intake (Perez-Vizcaino et al., 2009). It is naturally-occurring in fruits and vegetables, such as apples, cranberries and onions. It is also found in black tea, red wine and various fruit juices. In the United States, the consumption of flavonol glycosides which are expressed as quercetin equivalents are at levels of up to ~100 mg/day, the total flavonoids (including flavanones, flavones, flavonols, anthocyanins, catechins and biflavans) intake from a normal mixed diet is estimated as ~1g/day flavonoids (expressed as quercitrin equivalents, where one biflavan molecule is equal to 2 molecules of quercitrin) (Harwood et al., 2007).

Quercetin has the chemical structure of two benzene rings linked by a heterocyclic pyran or pyrone ring, and its chemical formula is 3,3',4'5,7-pentahydroxyflavone (Figure 1.2) (Harwood et al., 2007). The free hydroxyl groups and their mutual location determine the antioxidant activity of quercetin (Materska, 2008). The B-ring hydroxyl configuration shows highest scavenging capacity in scavenging of reactive oxygen species and reactive nitrogen species. A 3'4'-catechol structure in the B-ring is the most potent scavenger of lipid peroxidation (Heim et al., 2002).

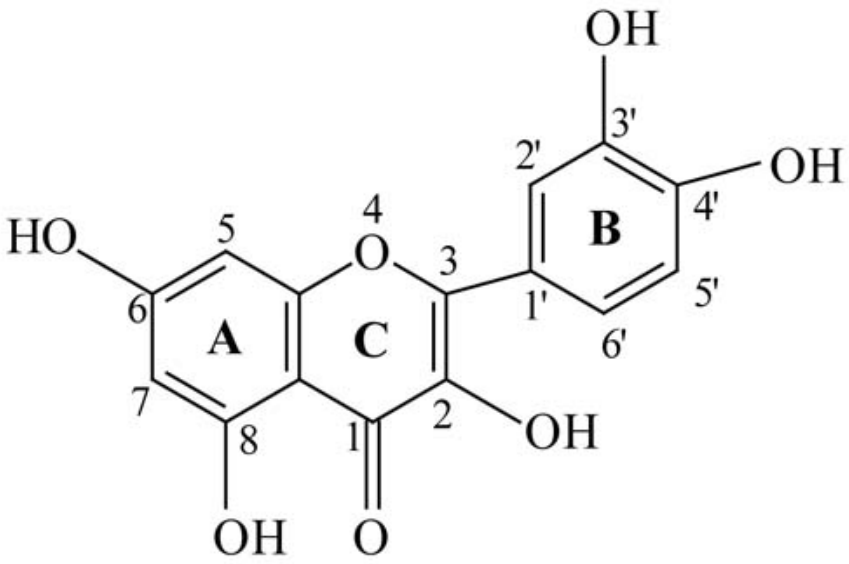

Figure 1.2. Chemical structure of quercetin.

Quercetin is among the most potent antioxidant of the polyphenols. It shows scancenging activity to hydrogen peroxide (H_2O_2), oxygen (O_2), as well as reactive nitrogen species (RNS) such as nitric oxide (NO) and peroxynitrite (cited in

Zimmerman et al., 2014). Additionally, quercetin exhibits numerous biological and pharmacological activities, such as cardioprotective, anti-mutagenic, antioxidant, anti-inflammatory, chelation, antilipoperoxidative, antiproliferative, anti-carcinogenic and anti-angiogenic (Harwood et al., 2007; Russo et al., 2012). Quercetin is therapeutically effective for hypertension (Perez-Vizcaino et al., 2009), skin oxidative stress (Inal & Kahraman, 2000; Joshan & Singh, 2013; Kimura et al., 2009; Manca et al., 2014), rheumatoid arthritis (Natarajan et al., 2010) and wound healing (Gomathi et al., 2003). In cancer treatment, quercetin also reacts as a multidrug resistance modulator and thus a potential chemosensitizer (Chen et al., 2010). In addition, quercetin has been shown to be chemopreventive and a possible solution for anthracycline-induced cardiotoxicity and multidrug resistance (Czepas & Gwoździński, 2014).

Long-term oral animal toxicity studies demonstrated the safety of dietary quercetin (Harwood et al., 2007).

1.2 Microencapsulation

1.2.1 Introduction of microencapsulation

Microencapsulation which has been developed since the 1950s is defined as a process of surrounding or enveloping the substance of either solids, liquids, or gaseous materials in a coating or capsule, yielding capsules ranging from sub-micron to several millimeters in size (Fang & Bhandari, 2010). The microencapsulation methods distinguishes the capsules in term of particle size ranges or denomination of either nanocapsules (size range smaller than 0.2 μm), microcapsules (size range between 0.2 and 5000 μm) or macrocapsules (size range larger than 5000 μm)

(Barbosa-Cánovas et al., 2005). The encapsulated substance is called core material, active ingredient or agent, fill, payload, internal phase or nucleus. On the other hand, the material encapsulating the core is called coating, membrane, shell, carrier or wall material. The coating materials can be sugars, gums, proteins, polysaccharides, lipids and synthetic polymers (Barbosa-Cánovas et al., 2005; Fang & Bhandari, 2010).

Several conformations of microcapsules can be produced for encapsulation. The three main conformations are: single particle structure (regular or irregular), aggregate structure and multi-walled structure. Single structure microcapsule is a sphere of the active ingredient surrounded by a thick uniform wall. An aggregate structure is asymmetrically and variably shaped, with several distinct core particles embedded throughout the microcapsule. This type of microcapsules may have multiple core structure. The multi-walled microcapsules have different concentric layers which either have the same, or quite different compositions (Gibbs et al., 1999; Sachan et al., 2006). Microcapsules also present in multi-core structure and matrix. Multi-core microcapsules have a number of different sized chambers within the shell (Kumar et al., 2011). Figure 1.3 shows various morphologies of microcapsules. The morphology of the internal structure of microcapsules is influenced by the encapsulation techniques, the types of core materials and coating materials used. Liquid or dispersion of core material to be encapsulated will result in perfect microcapsules rather than solid core (Sachan et al., 2006).

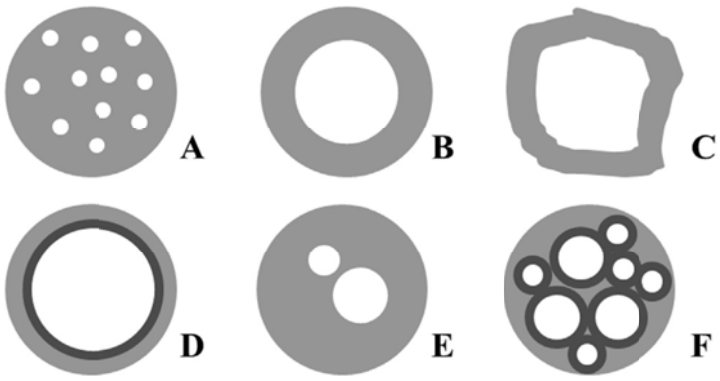

Figure 1.3. Schematic morphologies of different types of microcapsules: (A) matrix, (B) single structure microcapsule (regular), (C) irregular single structure microcapsule, (D) multiwall microcapsule, (E) multi-core microcapsule and (F) aggregate structure microcapsule. Adapted from de Azeredo (2005).

There are a wide variety of microencapsulation techniques or processes used in variety of industries. Briefly, these technologies can be classified into physical methods, physicochemical methods and chemical methods (Munin & Edwards-Lévy, 2011). The examples of each method are given as follows:

(i) Physical methods: spray drying, fluid bed coating, pan coating, extrusion, centrifugal extrusion;

(ii) Physicochemical methods: spray chilling and spray cooling, ionic gelation, solvent evaporation-extraction, hot melt coating, coacervation; and

(iii) Chemical methods: interfacial polycondensation, *in situ* polymerization, interfacial polymerization, interfacial crosslinking.

1.2.2 Core material

The core material which is the material to be coated to serve the specific purpose can be liquid or solid in nature. The composition of core material can be varied, such as liquids and dispersion forms for liquid core materials, while active constituents, stabilizers, diluents, excipients and release-rate retardants or accelerators are examples of solid core materials. The composition of core material is selected depending on the final microcapsules properties (Bansode et al., 2010; Sachan et al., 2006).

1.2.3 Coating material

A wide variety of coating materials are available for microencapsulation, depending on the material to be coated and the characteristics desired in the final microcapsules (Barbosa-Cánovas et al., 2005). Effective coating materials should meet the properties such as film forming, strength, pliable, tasteless, stable, non-hygroscopic, soluble in aqueous media, good rheological at high concentration and ease of manipulation during the process of encapsulation and optical properties. Furthermore, the selected coating material should be chemically compatible and nonreactive with the core material during processing and storage. Additionally, it should meet the requirement of the system such as microcapsules solubility properties and core material release properties (Bansode et al., 2010; Barbosa-Cánovas et al., 2005; Sachan et al., 2006). Examples of coating materials are as follows (Bansode et al., 2010):

(i) Water soluble resins: gelatin, gum arabic, starch, polyvinylpyrrolidone, carboxymethylenecellulose, hydroxyethylcellulose, methylcellulose, arabinogalactan, polyvinyl alcohol, polyacrylic acid;

(ii) Water insoluble resins: ethylcellulose, polyethylene, polymethacrylate, polyamide (nylon), poly (ethylenevinyl acetate), cellulose nitrate, silicones, poly(lactide-co-glycolide);

(iii) Waxes and lipids: paraffin, carnauba, spermaceti, beeswax, stearic acid, stearyl alcohol. Glyceryl stearates; and

(iv) Enteric resins: shellac, cellulose, acetate phthalate, zein.

1.2.3 (a) Gelatin

Gelatin is derived from the fibrous protein collagen by the process of partial hydrolysis; collagen which is broadly found as the major component of animal skin, bones and connective tissue (Karim & Bhat, 2009; Mukherjee & Rosolen, 2013). Depending on the hydrolysis process which is the method by which collagen is pretreated, two types of gelatin are available, namely, type A and type B gelatins (Karim & Bhat, 2009; Singh et al., 2002). Type A gelatin is derived from acid processed collagen (isoelectric point at pH 6-9), while type B gelatin is derived from alkaline processed collagen (isoelectric point at approximately pH 5) (Karim & Bhat, 2009). The acid or base precursor results in different characteristic features of gelatin due to different number of NH_2 and COOH groups on the gelatin molecules (Siow & Ong, 2013).

Collagen molecules are composed of three α-chains which consist of continuous repetitions of Gly-X-Y amino acid sequences where X is mostly proline and Y is mostly hydroxyproline (Eastoe & Leach, 1977), forming a triple-helix structure. The intertwined triple-helix adopts a 3D structure that provides an ideal geometry for inter-chain hydrogen bonds. The triple-helices are stabilized by the inter-chain hydrogen bonds (Duconseille et al., 2015; Karim & Bhat, 2009). Denaturation of collagen by thermal or physical and chemical means causes the destruction of hydrogen bonds, which results in breaking of the triple-helix structure into random coils to produce gelatin (Bigi et al., 2004; Karim & Bhat, 2009). Gelatin contains amino acids in varying composition as reported by Eastoe (1955). The amino acid composition of gelatin is very close to that of its parent collagen (Karim & Bhat, 2009).

Gelatin is biodegradable, non-toxic, and easy to crosslink and to modify chemically. It is frequently used in food, pharmaceutical, biomedical and photographic industries. It is commonly used as the main ingredient of hard and soft capsules, microspheres, sealants for vascular prostheses, wound dressing and adsorbent pad for surgical use and tissue regeneration. Gelatin is soluble in aqueous solution at temperature of about 40 °C and present in the sol state (Bigi et al., 2004). When gelatin is cooled below 30-35 °C the random coil polypeptide chains will undergo a conformational disorder-order transition and partly regenerate the collagen triple-helix structure and form thermoreversible gels by associating helices in junction zones stabilized by hydrogen bonds (Bigi et al., 2004; Strauss & Gibson, 2004). Because gelatin is soluble in aqueous solution, gelatin used as coating material or matrix of microcapsule products must be submitted to crosslinking, which improves both thermal and mechanical stability of the biopolymer (Bigi et al.,

2004). Crosslinking is important for the gelatin capsules to be insoluble at high temperatures, to reduce swelling in water and decrease permeability across cell membranes. Formaldehyde and glutaraldehyde are the most common agents used in gelatin crosslinking.

Gelatin is widely used as the main ingredient of the complex coacervation in the food and pharmaceutical industries (Comunian et al., 2013; Dong et al., 2011; Hanes et al., 2001; Jizomoto et al, 1993; Saravanan & Rao, 2010; Shinde Y Nagarsenker, 2011). The most important property of this protein is that gelatin is a polyampholyte with amine ($-NH_2$) and carboxyl (-COOH) functional groups along with hydrophobic groups (lurea Raţă et al., 2013). Gelatin is a random coil polymer carrying positively and negatively charged-sites in almost 1:1 ratio. Additionally, it is associated with a small persistence length of about 2 nm (Bohidar, 2008). In solution, gelatin can be ionized to either $–COO^-$ or - NH_3^+ depending on the pH of the solution. At pH above the isoelectric point, gelatin charged negatively; whereas at pH below the isoelectric point, gelatin charged positively. Hence, gelatin will react with oppositely charged biomolecules in the same medium via electrostatic interaction to form polyionic complexes (Young et al., 2005). For example, in a mixture containing gelatin (a protein) and an anionic polysaccharide, adjustment of the pH to below the isoelectric point (pI) or the electrical equivalence pH (IEP) of gelatin would result in maximum electrostatic attraction where the two biopolymers are carrying oppositely charge (Siow & Ong, 2013). For instance, complex coacervation occurred in a mixture of gum arabic (acacia) and type A gelatin at pH 4.5 (Bhattacharyya & Argillier, 2005; Siow & Ong, 2013), or occurred in a mixture of gum arabic (acacia) and type B gelatin at pH 3.5 (Siow & Ong, 2013). On the other hand, a gelatin-cationic polysaccharide system requires the adjustment of the mixture pH to above

the isoelectric point of gelatin for electrostatic attraction. For instance, complex coacervation occurred in a type B gelatin-chitosan system at pH 5.25-5.5 (Remuñán-López & Bodmeier, 1996). At pH 5.25-5.5, gelatin will be negatively charged (since the isoelectric point of gelatin B is 4.7-5.2) and it will electrostatically interact with positively charged chitosan to form an insoluble complex (complex coacervate). At such pH, gelatin-chitosan complex coacervation should be limited to type B gelatin. The isoelectric point of type A gelatin is typically 8-9, so its complex coacervation with chitosan should be limited to pH values above this (Thies, 2007). However, chitosan is precipitated at solution of pH higher than 6 since the pKa of chitosan is about pH 6.3 (Paños et al., 2008). Figure 1.4 shows the chemical structure of gelatin.

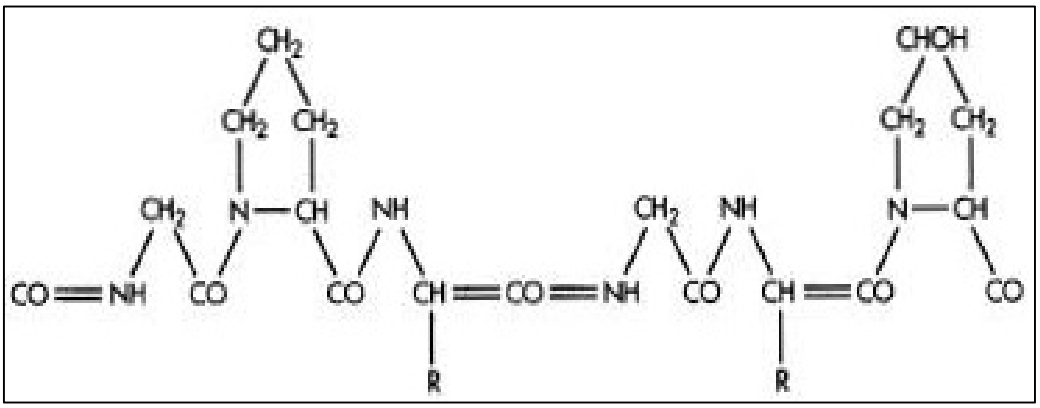

Figure 1.4. Chemical structure of gelatin.

1.2.3 (b) Chitosan

Chitosan is an amino-polysaccharide derived by alkaline deacetylation of chitin (an N-acetyl-glucosamine polymer). Chitin is the second most abundant polymer in nature after cellulose and is from crustaceans, exoskeleton of insects and fungi. Chitosan is a cationic polysaccharide, a copolymer of 2-acetamido-2-deoxy-β-D-glucose and 2-amino-2-deoxy-β-D-glucose units, and it differs in the degree of N-acetylation (40-98%) and molecular weight (50-2000 kDa) (Basu et al., 2010; Estevinho et al., 2013; Paños et al., 2008). The solubility of chitosan, which has a pKa value of 6.3 (Paños et al., 2008), depends closely on the degree of acetylation (Kumirska et al., 2011) where it is normally insoluble in aqueous solutions of pH value higher than pKa, however it is soluble in dilute acid solutions below pH 6.5 (Riva et al., 2011). The protonated free amino groups facilitate the solubility of the molecule and characterize chitosan as a cationic polyelectrolyte (Kumirska et al., 2011). The chemical structure of chitosan is shown in Figure 1.5.

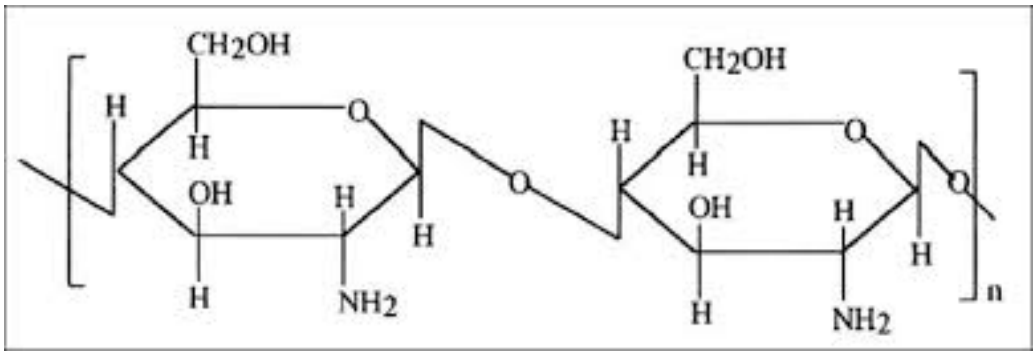

Figure 1.5. Chemical structure of chitosan.

Chitosan has been widely used in food, cosmetic and pharmaceutical industries as a carrier for drug delivery because it possesses excellent properties, such as non-toxicity, biodegradability, biocompatibility and absorption properties (Paños et al., 2008). Additionally, a large number of amine groups provide availability of chitosan interacting with other substances (Jaya et al., 2010). Since the 90's, chitosan microspheres have been used as controlled drug delivery systems for conventional drugs, protein drugs and bioactive compounds. Chitosan is particularly useful as coating material in microencapsulation for controlled release of bioactive compounds. Chitosan can establish covalent or ionic bonds with the crosslinking agents, for example, glutaraldehyde which form Schiff bases with amino groups building three dimensional network, thus increases the internal surface area for absorption and the encapsulated active substance stays retained, and consequently as controlled release carrier (Estevinho et al., 2013; Jaya et al., 2010). On the other hand, chitosan and its derivatives in microencapsulation of peptides and proteins have proven to enhance their permeation, since they have affinity for enzymes that usually degrade the peptide (e.g., insulin). Hence, the bioavailability of peptide drugs is increased due to permeation enhancement by chitosan, its enzyme inhibition and mucoadhesive properties (Paños et al., 2008).

Chitosan is a good coating material candidate for different microencapsulation techniques because its cationic properties in acidic conditions make it able to electrostatically interact with negatively charged molecules or polymers (Riva et al., 2011). Chitosan can form nanoparticles by ionic gelation with polyphosphates and with nucleic (Riva et al., 2011). In addition, chitosan is used for simple coacervation together with incompatible material, such as sodium sulphate. Simple coacervation is a simple and mild method, however, results in low encapsulation efficiency (Paños et

al., 2008). Chitosan is also used for complex coacervation with type B gelatin since one behaves cationic and the other behaves anionic in solutions at pH value above the isoelectric point of gelatin. Besides, complex coacervation between chitosan and the negatively charged lipid, lecithin has produced nanoparticles. Sodium alginate-chitosan systems have been widely studied. The release of albumin microencapsulated in this system is influenced by the molecular weight of chitosan used (Paños et al., 2008).

1.2.4 Crosslinking agent

Crosslinking is a process of hardening of microcapsules which can improve microcapsule stability via formation of covalent bonds between molecule chains to form a three-dimensional network of connected molecules. The crosslinking agents can be chemical or enzymatic, and usually are molecules with at least two reactive functional groups that allow the formation of bridges between polymeric chains by covalent bonds (Estevinho et al., 2013). Covalent crosslinking of microcapsules allows drug release by diffusion due to absorption of water and/or bioactive compounds instead of dissolution (Estevinho et al., 2013). Aldehydes such as glutaraldehyde, formaldehyde and glyceraldehye are the most commonly used chemical crosslinkers in microencapsulation of polymers which contain amino groups (Hernández-Muñoz et al., 2004b). However, due to the possible toxicity of chemical crosslinkers, enzymatic crosslinkers such as transgutaminase is usually applied in microencapsulation of food ingredients (De Jong & Koppelman, 2002; Dong et al., 2008).

1.2.4 (a) Formaldehyde crosslinking mechanism

Formaldehyde is a gas with molecular structure of HCHO. Formaldehyde dissolves rapidly in water and forms methylene hydrate, HO-CH_2-OH (Figure 1.6a). Methylene hydrate molecules react with one another in aqueous solution to form polymers (Figure 1.6b). Formaldehyde obtained in liquid form is called formalin, with 2-8 polymers and contains of 37-40% formaldehyde and 60-63% of water (by weight) (Kiernan, 2000).

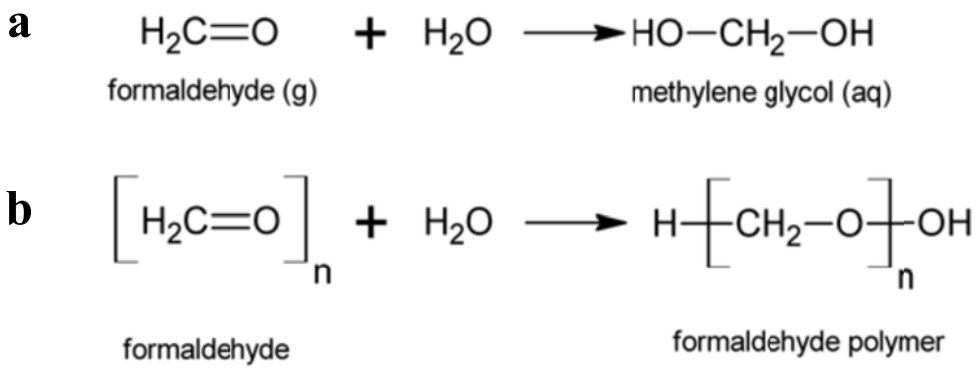

Figure 1.6. Formation of methylene glycol and formaldehyde polymer.

Gelatin and chitosan are both hydrophilic polymers, and are susceptible to aldehyde crosslinking to improve physical properties thus suitable for controlled release matrix. Free amino groups, such as ε-amine groups of lysine or hydroxylysine residues of gelatin and primary amine groups of chitosan, and also free carboxylic acid residues of aspartic and glutamic acid in the gelatin structure can react with aldehyde groups of aldehyde crosslinkers, for example, formaldehyde (Lai et al., 2010; Rose et al., 2014). The general formaldehyde crosslinking mechanism is: (1)

Aldehyde group of formaldehyde reacts with amine group of matrix leading to dehydration of the methylol intermediate to yield an active Schiff base. This is a fast process. (2) Following the polymerization of formaldehyde, the Schiff base reacts with another amine group to form cross-link $–CH_2-$ (methylene bridge) (Wu et al., 2011). The formation of methylene bridges proceeds much more slowly compared to the first step. In collagen crosslinking with formaldehyde, the crosslink most often occurs between the nitrogen atom at the end of the side-chain of lysine and the nitrogen atom of a peptide linkage (Figure 1.7) (Kiernan, 2000). Such number of crosslinks increases with time and can lead to an intermolecular and intramolecular crosslinking network (Kiernan, 2000). In addition, collagenous samples such as gelatin may form inter- and intramolecular crosslinks with cyclic structure within collagen fibers (Bigi et al., 2004).

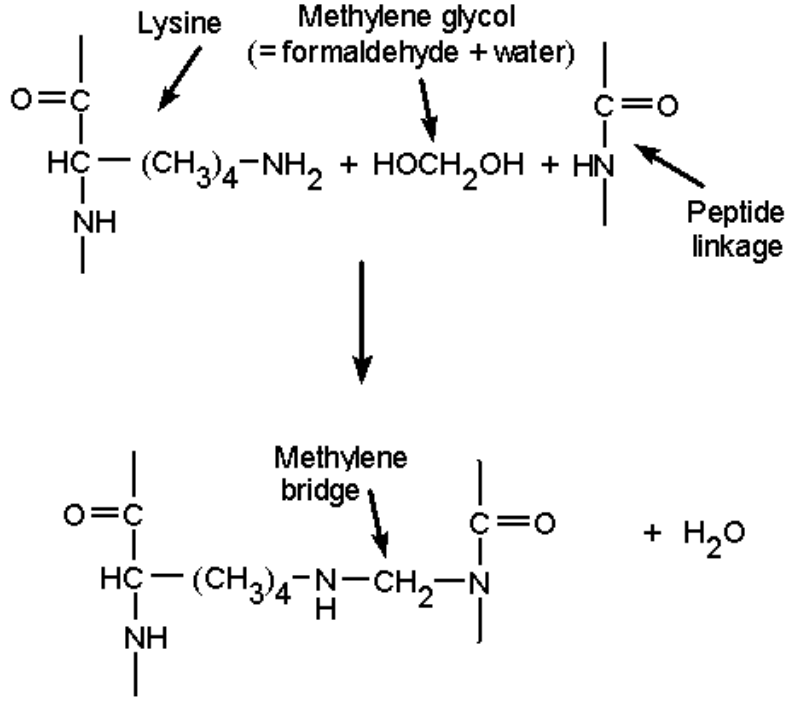

Figure 1.7. Formaldehyde crosslinking: formation of methylene glycol and methylene bridge. Adapted from Kiernan (2000).

1.2.5 Classification of microcapsules and microspheres

Microparticles can be classified according to their structure, namely, microcapsules and microspheres. Microcapsules consist of a polymeric shell (envelope or wall) and an encapsulated active product (core material) located within the shell. Thus, the core and the wall are well-defined in microcapsule systems. Microspheres are in strict sense, spherical empty particles because the drug substance is either homogeneously dissolved or dispersed in a polymeric matrix, thus no well-defined wall exists (Kumar et al., 2011; Kvitnitsky et al., 2005). In addition, for large size particles, microbeads, beads, spheres and spherical particles are also terms used alternatively for microcapsules and microspheres (Kvitnitsky et al., 2005). Figure 1.8 shows the morphologies of microcapsule and microspheres. Microspheres are essentially spherical in shape, whereas microcapsules may be spherical or irregular in shape.

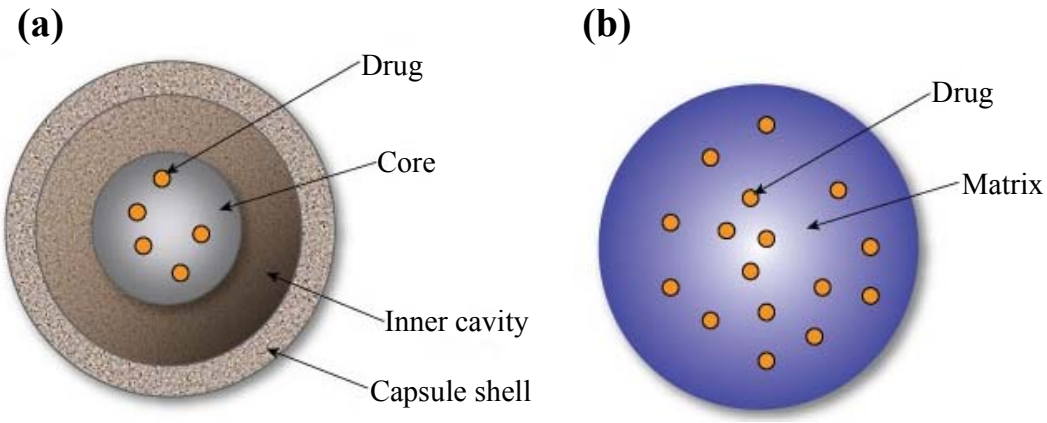

Figure 1.8. Schematic morphologies of (a) microcapsule and (b) microsphere. Adapted from Lembo and Cavalli (2010).

1.2.6 Coacervation microencapsulation

Coacervation encapsulation is a physiochemical process, and is classified as simple or complex. Simple coacervation systems only contain one colloidal solute (e.g., only gelatin), while in complex coacervation systems contain more than one solute (e.g., gelatin and gum acacia) (Barbosa-Cánovas et al., 2005). In general, this technology consists of three steps which are carried out under continuous agitation, that include: (1) formation of three immiscible chemical phases, (2) deposition of coating, and (3) rigidization of the coating. Briefly, the coacervation microencapsulation process is initiated by either changing the pH or temperature of the colloidal system, or adding a non-solvent or another complete chemical (e.g., sodium sulfate) to the colloidal system which contains the active ingredient (core material). Consequently, a two-phase system is created that consist of the colloid-rich phase (appearing as an amorphous cloud) and the colloid-poor phase/aqueous phase. Deposition of the newly formed coacervate phase around the active ingredient (core material) suspended or emulsified in the same reaction media forms small and still unstable microcapsules. Rigidization of the capsule wall can be done by crosslinking with chemical crosslinker (e.g., glutaraldehdye) or enzymatic crosslinker (e.g., transglutaminase), or by adjusting temperature or pH of the colloid system. The final steps of the process include collecting, washing and drying (Barbosa-Cánovas et al., 2005; Gouin, 2004; Sachan et al., 2006). This is a high payload microencapsulation technique, up to 99% with achievable yield (Gouin, 2004).

1.2.6 (a) Complex coacervation systems

Complex coacervation was first introduced by Bungenberg de Jong (1929) in their investigation for the system of gelatin-gum arabic. The name complex

coacervation is to distinguish from simple coacervation where the complex coacervation process involves the interaction of two oppositely charged polyelectrolytes as opposed to the simple coacervation that is based on single biopolymer. Complex coacervation is a liquid-liquid phase separation phenomenon that occurs as a consequence of electrostatic interaction between the two oppositely charged polyelectrolytes in a solution (Milanović et al., 2014). The neutralization of the opposite net charges of polyelectrolytes in the mixed solution separates the solution into a highly concentrated coacervate phase in the form of microdroplets and a dilute bulk phase (Bungenberg de Jong, 1949; Strauss & Gibson, 2004).

Complex coacervation may result in a mixture of oppositely charged polyelectrolytes (PE-PE) and polyelectrolytes with oppositely charged colloids (colloid-PE), such as micelles, proteins or dendrimers in aqueous media (Kizilay et al., 2011). Gelatin A-gelatin B and gelatin B-chitosan systems are examples of PE-PE and colloid-PE coacervations, respectively. Figure 1.9 illustrates the process of microencapsulation by complex coacervation.

1.2.6 (b) Complex coacervation microencapsulation process

The deposition of the coacervate onto the core droplets to form the microcapsule shell and maintain the integrity of shell and size depend on several processing parameters. These parameters include polymer type, molecular weight, charge density, concentration of polymers and their ratio, pH and temperature of the system, and cooling rate. Among these factors, pH of the coacervation system and polymers mixing ratio are the most studied factors in complex coacervation microencapsulation (Koh & Tucker, 2011; Liu et al., 2009; Shinde & Nagarsenker, 2009; Wang et al., 2014; Xiao et al., 2011). This is because improper mixing ratio of

oppositely charged polyelectrolyte can cause precipitation due to imbalance of charge density.

During the coacervation process, the temperature is above the melting point of colloid polymer (i.e., gelatin) under constant stirring, thus coacervate formed is initially a liquid. This allows the coacervate to engulf the dispersed core material droplets or particles, thereby coating them with a thin film of liquid coacervate. Thereafter, cooling of the coacervates below its gel temperature will settle the gel structure of the coacervate (Thies, 2007). For example, when gelatin gel is cooled below melt temperature results the random coil polypeptide chains link up to form collagen-like triple helices for part of their length (Strauss & Gibson, 2004). This transforms the thin liquid film that surrounds the small droplets of core material into a thin gel coating. The changes of temperature not only change the coacervate from liquid form to gel form, but also change the viscosity and rheology of the coacervate, thereby producing a major impact on the success of a complex coacervation encapsulation process (Thies, 2007). Crosslinking of microcapsules has improved its stability against mechanical force and modified drug release (Alvim & Grosso, 2010). Figure 1.10 illustrates the formation of microcapsules by coacervation.

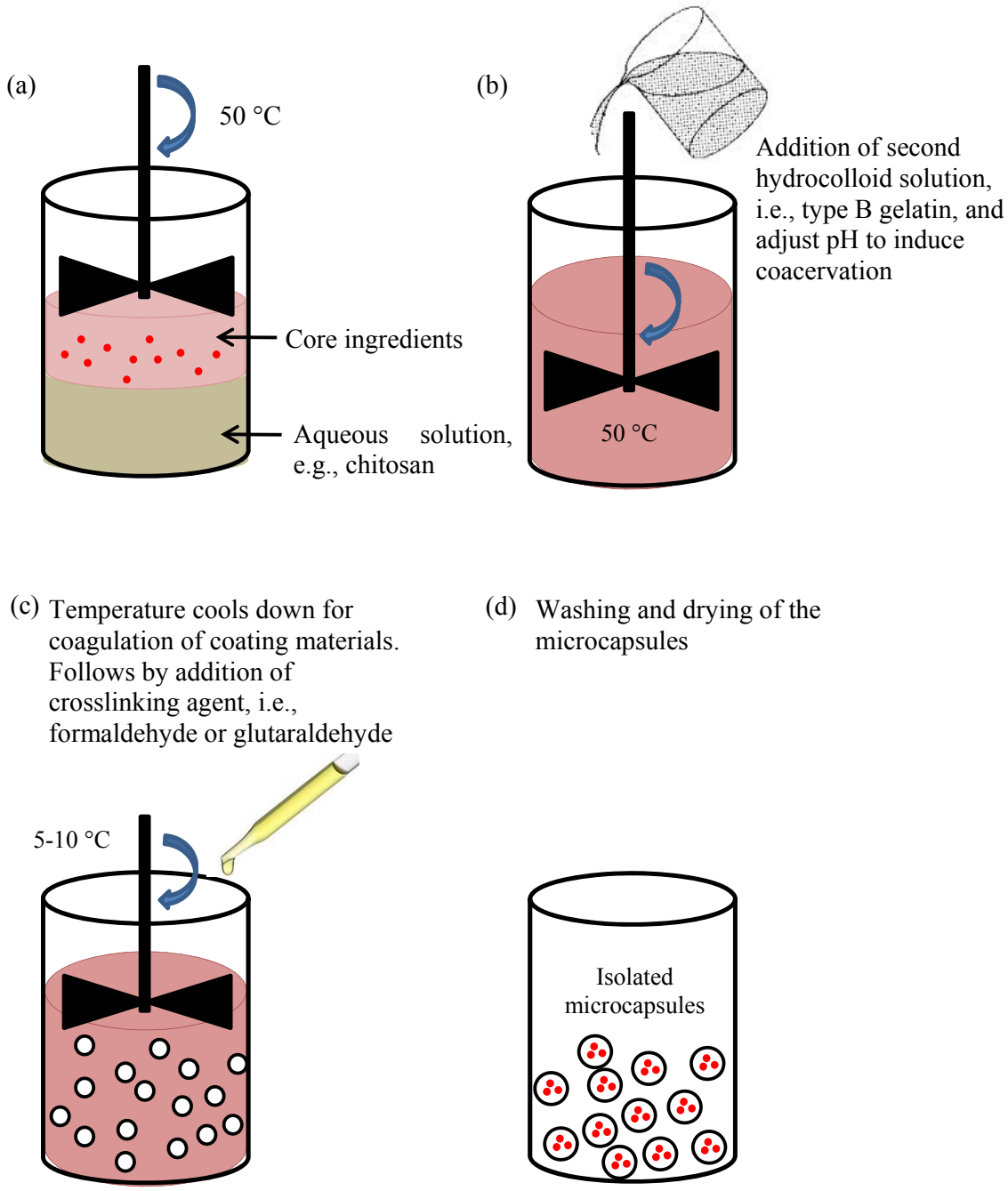

Figure 1.9. Process of microencapsulation by complex coacervation: (a) emulsification or suspension of core ingredients in the vehicle phase (typically aqueous solution); (b) induce complex coacervation by addition of a second complexing hydrocolloid; (c) solidification of wall materials and crosslink to stabilize the microcapsules; and (d) washing and drying.

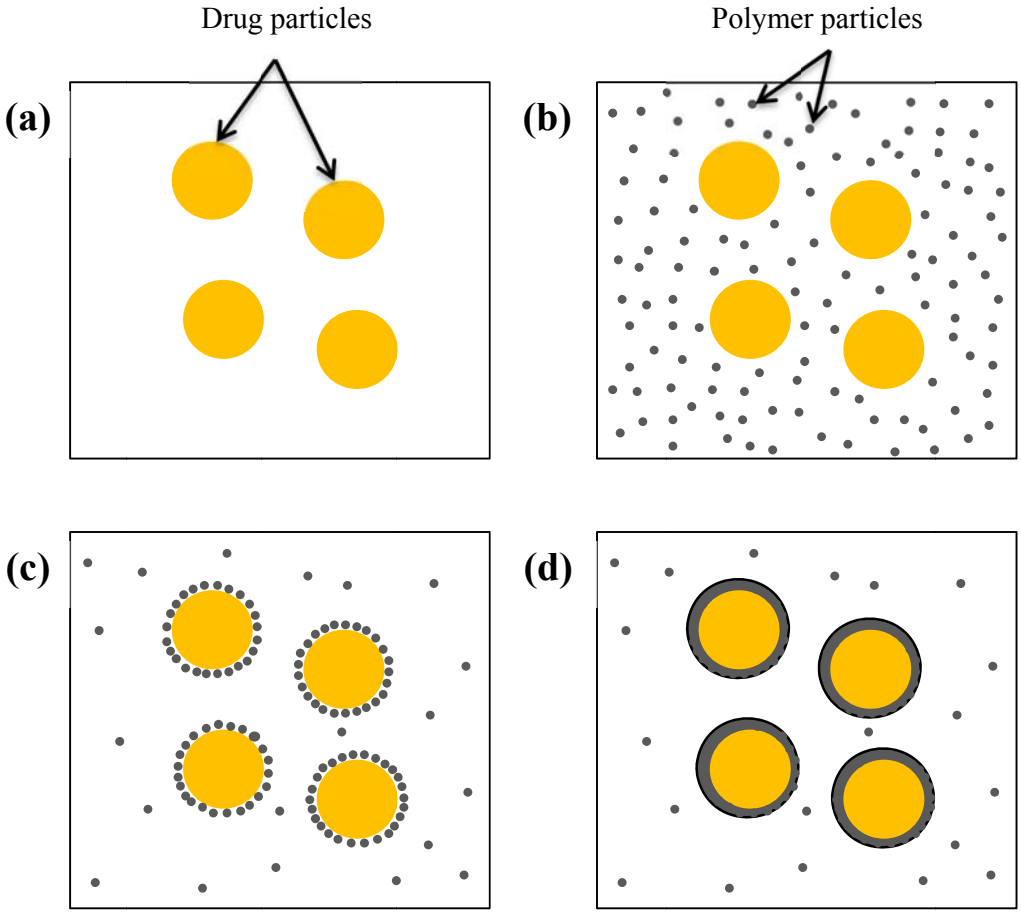

Figure 1.10. Schematic representation of microencapsulation by coacervation: (a) dispersed liquid or solid drug particles, (b) induction of phase separation, (c) deposition of microdroplets at the surface, and (d) fusion into a membrane.